

Solitary states in spiking oscillators with higher-order interactions

Vladimir V. Semenov,^{1,*} Subhasanket Dutta,² Stefano Boccaletti,^{3,4,5}

Charo I. del Genio,^{4,6,7} Sarika Jalan,² and Anna Zakharova⁸

¹*Department of Physics, Saratov State University,
Astrakhanskaya str. 83, 410012 Saratov, Russia*

²*Complex Systems Lab, Department of Physics, Indian Institute of Technology Indore, Indore 452020, India*

³*Sino-Europe Complexity Science Center, North University of China, Taiyuan 030051, China*

⁴*Institute of Interdisciplinary Intelligent Science, Ningbo University of Technology, Ningbo, China*

⁵*CNR – Institute of Complex Systems, Madonna del Piano 10, Sesto Fiorentino, Firenze 50019, Italy*

⁶*Institute of Smart Agriculture for Safe and Functional Foods and Supplements, Trakia University, Stara Zagora 6000, Bulgaria*

⁷*School of Mathematics, North University of China, 030051, Taiyuan, China*

⁸*Bernstein Center for Computational Neuroscience,
Humboldt-Universität zu Berlin, Philippstraße 13, 10115 Berlin, Germany*

We study a system of globally coupled FitzHugh-Nagumo oscillators with pairwise and second-order interactions, showing that the presence of higher-order interactions substantially affects the character of the transition between synchronous and asynchronous states driven by changes in coupling strength. In particular, we demonstrate that, around the synchronization transition, solitary states emerge due to the presence of second-order interactions. We also show that, in difference to the phenomenology observed in systems of phase oscillators, at low fixed pairwise coupling strengths, solitary states appear for both transition directions as the second-order interaction strength is varied, whereas for higher couplings they only occur in the forward direction, with the backwards one characterized by explosive desynchronization.

I. INTRODUCTION

In the past decade, the presence of higher-order interactions has been recognized as having a substantial impact on the behaviour of a large number of complex systems [1, 2]. Their effects are particularly relevant because in the general case they cannot be recovered via the superposition of pairwise interactions. This has revived interest in the study of the static and dynamical properties of the structures that represent them, namely hypergraphs and simplicial complexes [3–6].

The influence of higher-order interactions on collective dynamics has been investigated in particular depth for networks of oscillators, where their relation to phenomena such as synchronization and resonance has been well established [7–10]. In such systems, one of their most striking effects is that they can give rise to abrupt *desynchronization* transitions in the absence of abrupt *synchronization* counterparts. Additionally, they can induce extreme multistability, whereby infinitely many stable and partially synchronized states coexist [11]. Such coexistence relates to the remarkable phenomenon of solitary states, in which one or more dynamical units split off and behave differently from the others despite the coupling being homogeneous [12–15].

Classically, solitary states appear at the edge of synchrony along the desynchronization path, and can be precursors for the emergence of chimera states [16, 17]. Their characteristic dynamical features are largely determined by the coupling properties. For example, in the presence

of adaptive coupling, the transition to desynchronization accompanied by the appearance of solitary states can occur via the emergence of multiclusters with hierarchical structure in cluster size [18, 19]. Also, in globally coupled networks of excitable systems, where repulsion dominates over attractive interactions, solitary states in non-locally coupled arrays inherit their dynamical properties from unbalanced periodic two-cluster states [20].

Notably, the formation of chimera states can also be an effect of the partial synchronization caused by higher-order interactions [21], which are additionally known to induce abrupt synchronization transitions with hysteresis and bistability of synchronized and incoherent states [22, 23], ultimately causing explosive synchronization [24]. However, these complex dynamical behaviours have so far been observed and studied only in networks of phase oscillators.

In this article, we show how higher-order interactions have a significant effect also on the transitions occurring in globally coupled systems of spiking oscillators. More specifically, we show how higher-order interactions cause the emergence of solitary states in both directions along the route to and from synchronization. We then characterize the specific effects of the different orders of interaction on the phenomenology of these systems.

II. THE MODEL

We study a system of globally coupled FitzHugh-Nagumo oscillators in the presence of both pairwise and second-order interactions. Its general evolution is de-

* semenov.v.v.ssu@gmail.com

scribed by the following system:

$$\begin{aligned} \varepsilon \dot{x}_i &= x_i - \frac{x_i^3}{3} - y_i + \frac{\sigma_p}{N} \sum_{\substack{j=1 \\ j \neq i}}^N \tanh(x_j - x_i) \\ &+ \frac{\sigma_h}{2N^2} \sum_{\substack{j=1 \\ j \neq i}}^N \sum_{\substack{k=1 \\ k \neq j}}^N \tanh(x_j + x_k - 2x_i), \\ \dot{y}_i &= x_i + a_i - by_i. \end{aligned} \quad (1)$$

Here, x_i and y_i are the state variables of the i th oscillator, the parameter $\varepsilon \ll 1$ is responsible for the time scale separation of the state variables, N is the number of oscillators, and σ_p and σ_h are the strengths of pairwise and higher-order interactions, respectively. We consider the system in Eq.(1) in the particular case of $b = 0$, so that the equations are akin to those of a van der Pol model. Note that, in this interpretation, ε is the inverse of the nonlinear damping. Furthermore, we consider the oscillators to be slightly different from each other, by imposing that a_i be random variables following a normal distribution with mean 0.5 and variance 0.001.

The model as defined involves nonlinear couplings in terms of the tanh function. This specific choice allows one to account for a saturation effect for large values of the function argument, a behaviour that is often desired when modelling biological processes such as neural cell dynamics [25, 26]. Additionally, the use of the hyperbolic tangent is quite convenient for a twofold reason. First, we cannot use a linear coupling to model higher-order interactions, as any linear function would factor into a sum of traditional pairwise couplings:

$$\sum_{\substack{j,k=1 \\ i \neq j \neq k}}^N (\alpha_j x_i + \alpha_j x_j + \alpha_k x_k) = \sum_{\substack{j=1 \\ j \neq i}}^N \left(\alpha_j x_j + \frac{\alpha_i}{2} x_i \right) + \sum_{\substack{k=1 \\ k \neq i}}^N \left(\alpha_k x_k + \frac{\alpha_i}{2} x_i \right). \quad (2)$$

Moreover, close to 0, the hyperbolic tangent is equal to the identity up to second order. Thus, when complete synchronization is achieved and the differences between the states of the oscillators almost vanish, the effect of the coupling is well approximated by a linear interaction, allowing one to apply powerful analytical methods to investigate the phenomena observed.

We study the system via numerical simulations, using $N = 100$ oscillators and $\varepsilon = 0.01$, starting from uniformly distributed random initial conditions $x_i \in [-1.5, 1.5]$ and $y_i \in [-1, 1]$. The steady state of a run for a given value of the coupling strengths is used as the initial state of the next run. At every time step, we compute the value of the order parameter $r(t) = \frac{1}{N} \left| \sum_{i=1}^N e^{i\theta_i} \right|$, where $\theta_i = \arctan(\frac{y_i}{x_i})$ is the angle of the i th oscillator. The range of the time-averaged order parameter $\langle r \rangle$, averaged over

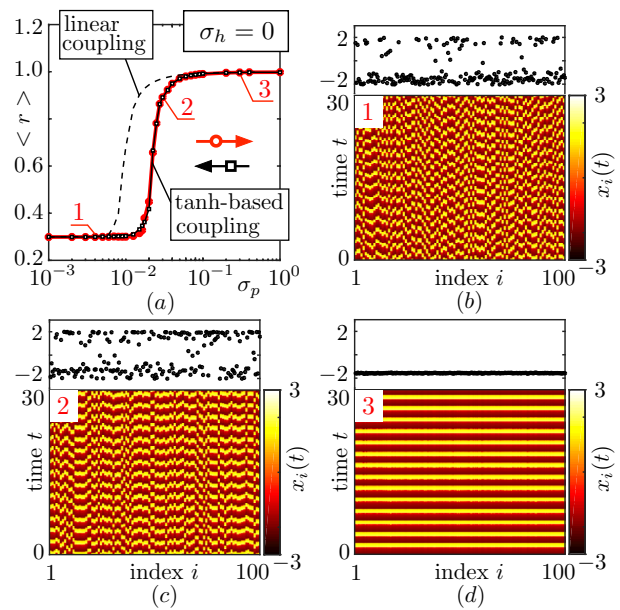


Figure 1. The transition to synchronization is continuous in the absence of higher-order interactions. (a) The time-averaged order parameter $\langle r \rangle$ changes continuously with the two-body interaction strength σ_p . The forward curve (solid red line) and the backwards one (solid black line) can be superimposed, and no hysteresis cycle occurs. The character of the transition remains the same if one uses a linear coupling, rather than the nonlinear one of Eq. (1) (dashed black line). Note the logarithmic scale for σ_p . (b)–(d) Space-time snapshots of the system, taken at the points 1–3 in panel (a), illustrate how, as σ_p increases above a critical value, the oscillators achieve global synchronization. In these panels, point 1 corresponds to $\sigma_p = 0.004$, point 2 to $\sigma_p = 0.02$ and point 3 to $\sigma_p = 0.4$. The upper insets show the final states of the system, which are used in the simulations as the initial conditions for the next points.

the steady state of the system, is between 0 and 1, with 0 corresponding to an asynchronous state, and 1 to fully synchronized oscillations. Additionally, we also compute the mean phase velocity for each oscillator, $\omega_i = 2\pi \frac{M_i}{\Delta T}$, where M_i is the number of complete rotations around the origin performed by the i th oscillator during a time interval of size ΔT .

III. RESULTS

A. Exclusively pairwise interactions

We start by considering a system with only pairwise interaction, i.e., with $\sigma_h = 0$. In such a case, a continuous transition between synchronous and asynchronous dynamics occurs as a function of the interaction strength. As shown in Fig. 1 (a), no hysteresis appears in the time-averaged order parameter, and the forward and backward curves are superimposable. The space-time snapshots of the system, shown in Fig. 1 (b)–(d), illustrate the transi-

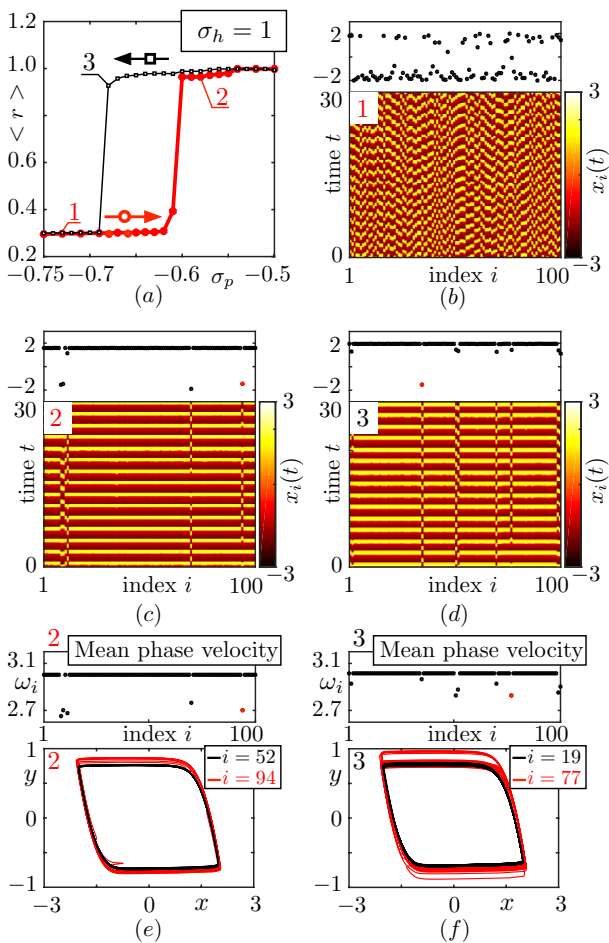


Figure 2. Higher-order interactions make the synchronization transition discontinuous and induce solitary states. (a) A hysteresis cycle appears in the transition to synchronization: the system switches to a synchronized state at $\sigma_p = -0.6$ (red line), but it reverts back to the asynchronous state only when σ_p is lowered to -0.69 (black line), indicating that the transition is first-order. (b)–(d) Space-time snapshots of the system, taken at the points 1–3 in panel (a), show the appearance of solitary states on the route to synchronization and to desynchronization. In these panels, point 1 corresponds to $\sigma_p = -0.73$, point 2 to $\sigma_p = -0.58$ and point 3 to $\sigma_p = -0.68$. The upper insets show the final states of the system, which are used in the simulations as the initial conditions for the next points. (e)–(f) The phase portraits of the synchronized oscillators (black) are limit cycles, whereas those of the oscillators corresponding to the solitary state (red) are open trajectories. The upper insets show the mean phase velocities of each individual oscillator. Panel (e) corresponds to point 2 and panel (f) to point 3.

tion to synchronization, with all the oscillators evolving in-phase for σ_p greater than a critical value.

Note that the nonlinearity of the coupling does not have a profound impact on the transition regime. In fact, as shown in Fig. 1 (a), the only effect caused by the specific functional form of the coupling is merely a shift of the curve of $\langle r \rangle$ as a function of σ_p .

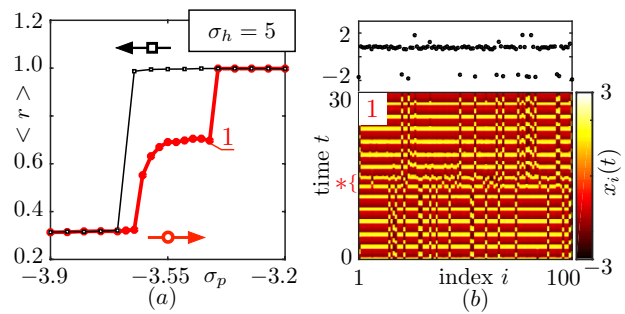


Figure 3. Stronger higher-order interactions suppress solitary states during the transition to desynchronization. (a) When σ_h is increased to 5, solitary states no longer appear in the backward transition (black line), whereas they still do in the forward one (red line), where they are a larger fraction than at lower values of σ_h . (b) The time evolution of the system at the point 1 in panel (a), corresponding to $\sigma_p = -3.425$, shows that, when solitary states appear, the specific oscillators that belong to them may change in time, while leaving their number unaltered. The moment of one such change is marked with a *. The upper inset shows the final state of the system.

B. Impact of second-order interactions

When three-body interactions are introduced in the system, a hysteresis cycle, shown in Fig. 2 (a), appears in the transitions between synchronous and asynchronous states. This indicates that the transition is no longer critical, but rather it is a first-order one, and the possibility of coexistence of stable incoherent and synchronized states is expected. We note, however, that the forward and backwards transitions are both accompanied by the occurrence of partial synchronization with the appearance of solitary states, as shown in Fig. 2 (b)–(d).

This shows that, as σ_p increases beyond the transition point, the system does not switch directly to global synchronization. Rather, an initial regime of partial synchronization is reached such that most oscillators are in phase, while the rest are not synchronized. Eventually, when σ_p increases further, the oscillators achieve complete synchronization. The behaviour is qualitatively unchanged, but reversed, when studying the backwards transition. Notably, the solitary states are stable, and they occur over a range of values of σ_p , showing their robustness.

The solitary states are also characterized by outliers in the mean phase velocities, as shown in Fig. 2 (e)–(f). Moreover, the phase portraits of the synchronized oscillators differ from those of the ones corresponding to solitary states. Specifically, the former are limit cycles, whereas the latter are slightly irregular, non-closed trajectories.

As the strength of higher-order interactions increases, the forward and backward transitions exhibit a dramatic change in behaviour. On the one hand, the desynchronization transition becomes completely abrupt, with the suppression of any solitary state, as shown in Fig. 3. On the other hand, the forward transition still features soli-

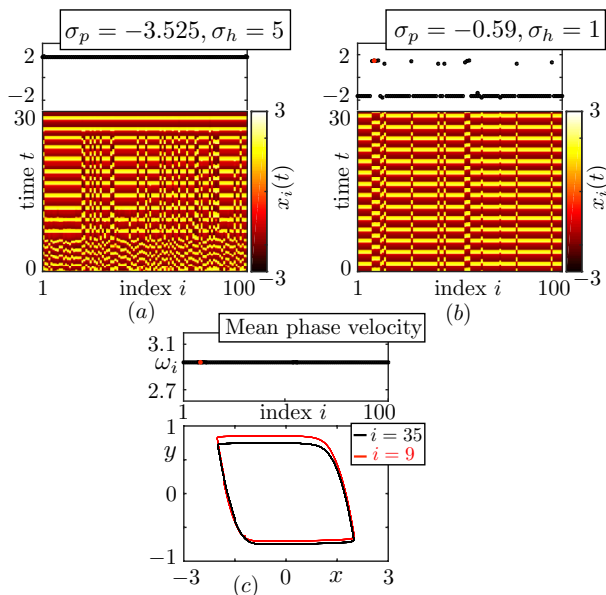


Figure 4. **Solitary states occur also for identical oscillators.** (a)-(b) Space-time snapshots of the system with identical oscillators at different values of σ_p and σ_h show the appearance of stable solitary states that evolve towards complete synchronization if the interaction strengths are sufficiently high. The upper insets show the final states of the system. (c) The phase portrait of an oscillator in the synchronized state (black) differs from that of one in the solitary state (red), even though their mean phase velocity is the same (upper inset). The parameters have the same values as in panel (b).

tary states, but with fundamentally different properties. In particular, the specific oscillators that participate in the solitary states changes over time. This is in stark contrast to what happens at lower values of σ_h , where, instead, the oscillators that constitute the solitary state remain unchanged. Note that the occurrence of such a change of dynamical regime of some oscillators does not significantly affect the fraction of asynchronous ones. As a result, the value of the time-averaged order parameter does not undergo large fluctuations as time progresses.

A further remarkable feature of the transition to synchronization shown in Fig. 3 (a) consists in the emergence of an intermediate state with $\langle r \rangle \approx 0.7$, which is stable for a range of coupling strengths $\sigma_p \in [-3.55, -3.425]$. The transition to synchronization finally occurs discontinuously at $\sigma_p \approx -3.4$. This effect is very reminiscent of the single-step first-order transitions accompanied by heterogeneous nucleation in adaptive dynamical networks [27, 28].

To confirm that the solitary states are not just an artifact due to the inhomogeneity of a system of non-identical oscillators, we study the system when all the oscillators are forced to be identical, which corresponds to imposing $a_i = 0.5$. The snapshot shown in Fig. 4 (a) shows that, at sufficiently high σ_p and σ_h , the solitary state eventually evolves into complete synchronization. However, at lower

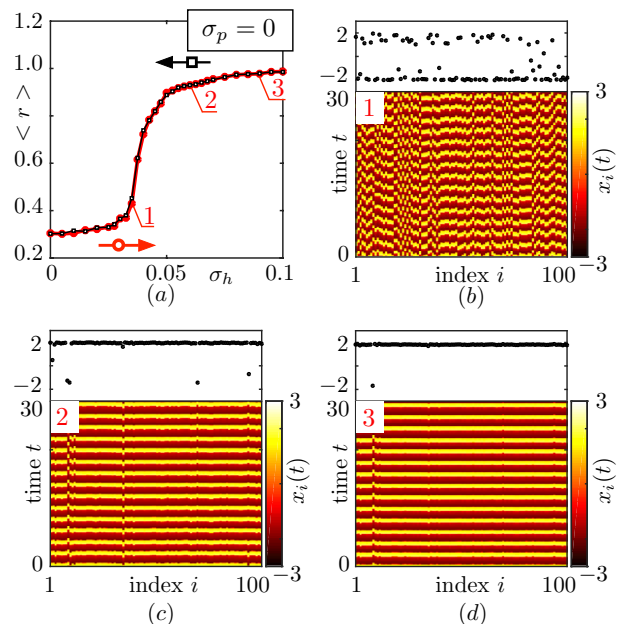


Figure 5. **Solitary states are a higher-order effect.** (a) The synchronization transition in the absence of pairwise interactions is continuous, with the forward curve (red) and the backwards one (black) that are superimposable. (b)-(d) Space-time snapshots of the system, taken at the points 1–3 in panel (a), illustrate the appearance of solitary states. In these panels, point 1 corresponds to $\sigma_h = 0.0375$, point 2 to $\sigma_h = 0.06$ and point 3 to $\sigma_h = 0.09$. The upper insets show the final states of the system, which are used in the simulations as the initial conditions for the next points.

values of the interaction strengths, the solitary states are stable in time, as shown in Fig. 4 (b). Similarly to the case of non-identical oscillators, the phase portraits of the attractors corresponding to the synchronized state and those in the solitary one, depicted in Fig. 4 (c), differ from each other. However, their mean phase velocities are the same, unlike what happens when the oscillators are not identical, and similarly to the states first reported in Ref. [20]. This phenomenology allows us to conclude that the occurrence of solitary states does not depend on the existence of dynamical differences amongst the oscillators, but rather it is a result of the presence of higher-order interactions in the system.

To better understand the role of both orders of interaction, we then consider the system in the absence of pairwise interactions, which corresponds to $\sigma_p = 0$. In this case, the results reported in Fig. 5 (a) show that the synchronization transition is continuous, with no bistability or hysteresis cycle. Nonetheless, solitary states still do occur, as evidenced by the the space-time snapshots in Fig. 5 (c)–(d), which strongly suggest that their appearance is inherently a higher-order effect, rather being caused by the simultaneous presence of first-order and second-order interactions.

To verify whether the phenomenology observed can be ascribed to finite-size effects, we study the synchroniza-

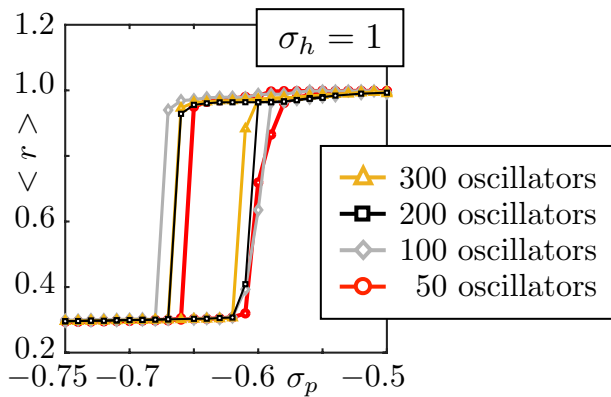


Figure 6. **The character of the synchronization transition is unaffected by system size.** Systems with different numbers of oscillators still undergo a first-order transition to synchronization, and the only changes are minor shifts in the transition points.

tion transition for different system sizes. This is particularly relevant since, in networks with higher-order interactions, this transition has been recently reported to be strongly affected by stochastic fluctuations for small system sizes [29]. In our case, the number of oscillators in the system only causes minor qualitative changes in the transition, but its first-order character, shown in Fig. 6, and the presence of solitary states remain unchanged.

IV. CONCLUSIONS

The interplay of pairwise and second-order interactions in systems of oscillators allows the occurrence of abrupt transitions between the synchronized regime and the asynchronous one, with the presence of hysteresis and bistability whereby both coherent and incoherent states coexist. Previously, such effects were investigated in networks of phase oscillators, which are one of the simplest model for studying synchronization. Here, we have shown how these transitions can occur also in the presence of more complex dynamics, using a system of FitzHugh-Nagumo oscillators as a case study.

Additionally, we have shown how solitary states can appear in either transition direction under specific circumstances. These happen in systems of identical and non-identical elements, and they occur regardless of the strength of the pairwise interactions. In fact, they still emerge even when two-body interactions are entirely neglected. Conversely, in the absence of higher-order interactions, solitary states are suppressed. This indicates that such states are an inherent higher-order effect in spiking oscillators, and they are not associated with the homogeneity of the system or with its size. Note that, unlike solitary states that were previously reported on an example of coupled phase oscillators [11], which always appear only in the forward transition, those we studied here can occur in both the transition to synchronization

and in that to desynchronization, provided that the coupling strengths are below a critical value.

A question that arises naturally is that of the type of the dynamics of the solitary states. Here, we analyzed phase portraits and trajectories obtained from different initial conditions. This allows us to state that small changes in initial conditions yield differences in the solitary state trajectories that become larger over time. For this reason, we suspect the solitary state dynamics to be chaotic. However, a rigorous answer to the question of the character of the solitary states would require a deeper study involving the analysis of Lyapunov exponents and correlation function, which we intend to carry out in the near future.

A related question is that of the dynamical relation between the solitary states we observe and synchronization. In our case, the solitary states coexist with the synchronous state and, in this sense, the observed regimes are fully consistent with classical solitary states. Therefore, it would be possible, in principle that their dynamics be actually transient, and that they eventually collapse onto a fully synchronous state. In our study, we have observed that the solitary states can disappear and arise again involving the same oscillators. Thus, we can conclude that they represent a robust oscillatory regime and correspond to a particular attractor. We plan to carry out a more detailed analysis of these aspects in future works, since it will require the study of stochastic dynamics to check their robustness against random perturbations, and of the differences of evolution caused by changes in the initial conditions to identify the basins of attraction.

Concluding, our results constitute a step forward in the understanding of solitary states and provide an additional piece of evidence for the existence of inherently higher-order effects. Note that solitary states in spiking oscillators are usually discussed in the context of pairwise interactions, often with nonlocal [20, 30] and global [17] couplings. Focusing on higher-order effects, our research complements the existing studies, providing observations of solitary states in systems with interactions beyond pairwise. Relating multi-body interactions with critical phenomena and dynamical transitions, our work highlights the relevance of accounting for higher-order networks when modelling complex systems.

ACKNOWLEDGEMENTS

V.S. acknowledges support by the Russian Science Foundation (project No. 24-72-00054). S.B. and S.J. acknowledge VAJRA grant VJR/2019/000034. S.B. also acknowledges support from the project No. PGR01177 of the Italian Ministry of Foreign Affairs and International Cooperation. C.I.D.G. acknowledges funding from the Bulgarian Ministry of Education and Science, under Project No. BG-RRP-2.004-0006-C02.

-
- [1] F. Battiston, G. Cencetti, I. Iacopini, V. Latora, M. Lucas, A. Patania, J.-G. Young and G. Petri, *Phys. Rep.* **874**, 1 (2020).
- [2] F. Battiston and G. Petri, *Higher-order systems*, Springer (2022).
- [3] S. Boccaletti, P. De Lellis, C. I. del Genio, K. Alfaro-Bittner, R. Criado, S. Jalan and M. Romance, *Phys. Rep.* **1018**, 1 (2023).
- [4] Y.-J. Ma, Z.-Q. Jiang, F. Fang, C. I. del Genio and S. Boccaletti, *Phys. Rev. E* **111**, 044304 (2025).
- [5] F. Parastesh, M. Mehrabbeik, K. Rajagopal, S. Jafari, M. Perc, C. I. del Genio and S. Boccaletti, *Phys. Rev. Research*, **7**, 033039 (2025).
- [6] C. I. del Genio, *Phys. Rev. Research* **7**, 033045 (2025).
- [7] A. Tlaie, I. Leyva and I. Sendiña-Nadal, *Phys. Rev. E* **100**, 052305 (2019).
- [8] L. Gallo, R. Muolo, L. V. Gambuzza, V. Latora, M. Frasca and T. Carletti, *Commun. Phys.* **5**, 263 (2022).
- [9] F. Parastesh, M. Mehrabbeik, K. Rajagopal, S. Jafari and M. Perc, *Chaos* **32**, 013125 (2022).
- [10] V. V. Semenov, *Eur. Phys. J. Spec. Top.*, <https://doi.org/10.1140/epjs/s11734-025-01567-2> (2025).
- [11] P. S. Skardal and A. Arenas, *Phys. Rev. Lett.* **122**, 248301 (2019).
- [12] P. Jaros, S. Brezetsky, R. Levchenko, D. Dudkowski, T. Kapitaniak and Y. Maistrenko, *Chaos* **28**, 011103 (2018).
- [13] S. Majhi, T. Kapitaniak and D. Ghost, *Chaos* **29**, 013108 (2019).
- [14] F. Hellmann, P. Schultz, P. Jaros, R. Levchenko, T. Kapitaniak, J. Kurths and Y. Maistrenko, *Nat. Commun.* **11**, 582 (2020).
- [15] L. B. Schülen, D. A. Janzen, E. S. Medeiros and A. Zakharova, *Chaos Soliton. Fract.* **145**, 110670 (2021).
- [16] P. Jaros, Y. Maistrenko and T. Kapitaniak, *Phys. Rev. E* **91**, 022907 (2015).
- [17] L. Schülen, A. Gerdes, M. Wolfrum and A. Zakharova, *Phys. Rev. E* **106**, L042203 (2022).
- [18] R. Berner, A. Polanska, E. Schöll and S. Yanchuk, *Eur. Phys. J. Special. Topics.* **229**, 2183-2203 (2020).
- [19] R. Berner, S. Vock, E. Schöll and S. Yanchuk, *Phys. Rev. Lett.* **126**, 028301 (2021).
- [20] I. Franović, S. Eydám, N. Semenova and A. Zakharova, *Chaos* **32**, 011104 (2022).
- [21] S. Kundu and D. Ghosh, *Phys. Rev. E* **105**, L042202 (2022).
- [22] P. S. Skardal and A. Arenas, *Commun. Phys.* **3**, 218 (2020).
- [23] A. D. Kachhval and S. Jalan, *Phys. Rev. E* **105**, L062203 (2022).
- [24] S. Boccaletti, J. A. Almendral, S. Guan, I. Leyva, Z. Liu, I. Sendiña-Nadal, Z. Wang and Y. Zou, *Phys. Rep.* **660**, 1 (2016).
- [25] M. Snipas, T. Kraujalis, K. Maciunas, L. Kraujaliene, L. Gudaitis and V. Verselis, *Biophys. J.* **119**, 1640 (2020).
- [26] F. Hejri, M. Veletić and I. Balasingham, *IEEE Access* **9**, 61114 (2021).
- [27] J. Fialkowski, S. Yanchuk, I. M. Sokolov, E. Schöll, G. A. Gottwald and R. Berger, *Phys. Rev. Lett.* **130**, 067402 (2023).
- [28] A. Yadav, J. Fialkowski, R. Berger, V. K. Chandrasekar and D. V. Senthikumar, *Phys. Rev. E* **109**, L052301 (2024).
- [29] A. Suman and S. Jalan, *Chaos* **34**, 101101 (2024).
- [30] E. Rybalova, V.S. Anishchenko, G.I. Strelkova and A. Zakharova, *Chaos* **29**, 071106 (2019).